Lower bounds and series for the ground-state entropy of the Potts antiferromagnet on Archimedean lattices and their duals

Robert Shrock* and Shan-Ho Tsai†
Institute for Theoretical Physics, State University of New York at Stony Brook, Stony Brook, New York 11794-3840
(Received 12 May 1997)

We prove a general rigorous lower bound for $W(\Lambda,q)=\exp[S_0(\Lambda,q)/k_B]$, the exponent of the ground-state entropy of the q-state Potts antiferromagnet, on an arbitrary Archimedean lattice Λ. We calculate large-q series expansions for the exact $W_r(\Lambda,q)=q^{-1}W(\Lambda,q)$ and compare these with our lower bounds on this function on the various Archimedean lattices. It is shown that the lower bounds coincide with a number of terms in the large-q expansions and hence serve not just as bounds but also as very good approximations to the respective exact functions $W_r(\Lambda,q)$ for large q on the various lattices Λ. Plots of $W_r(\Lambda,q)$ are given and the general dependence on lattice coordination number is noted. Lower bounds and series are also presented for the duals of Archimedean lattices. As part of the study, the chromatic number is determined for all Archimedean lattices and their duals. Finally, we report calculations of chromatic zeros for several lattices; these provide further support for our earlier conjecture that a sufficient condition for $W_r(\Lambda,q)$ to be analytic at $1/q=0$ is that Λ is a regular lattice. [S1063-651X(97)11410-6]

PACS number(s): 05.20.−y, 64.60.Cn, 75.10.Hk

I. INTRODUCTION

Nonzero ground-state disorder and associated entropy $S_0\neq 0$ is an important subject in statistical mechanics. One physical example is provided by ice, for which the residual molar entropy is $S_0=0.82\pm 0.05$ cal/(K mole), i.e., $S_0/R=0.41\pm 0.03$, where $R=N_{Avog}k_B$ [1–4]. Indeed, residual entropy at low temperatures has been observed in a number of substances, including nitrous oxide, NO, carbon monoxide, CO, and $FClO_3$ (a comprehensive review is given in Ref. [3]). In these examples, the entropy occurs without frustration, i.e., the configurational energy can be minimized. In magnetic systems, two examples are provided by the Ising antiferromagnet on the triangular and kagomé lattices [5,6]; here the ground-state entropy does involve frustration. A particularly simple model exhibiting ground state entropy without the complication of frustration is the q-state Potts antiferromagnet (AF) [7] on a lattice Λ, for $q\geq\chi(\Lambda)$, where $\chi(\Lambda)$ denotes the minimum number of colors necessary to color the vertices of the lattice such that no two adjacent vertices have the same color. As is already evident from the foregoing, this model also has a deep connection with graph theory in mathematics [8–12] since the zero-temperature partition function of the above-mentioned q-state Potts antiferromagnet on a lattice Λ satisfies $Z(\Lambda,q,T=0)_{PAF}=P(\Lambda,q)$, where $P(G,q)$ is the chromatic polynomial expressing the number of ways of coloring the vertices of a graph G with q colors such that no two adjacent vertices (connected by a bond of the graph) have the same color; hence the ground-state entropy per site is given by $S_0/k_B=\ln W(\Lambda,q)$, where $W(\Lambda,q)$, the ground-state degeneracy per site, is

$$W(\Lambda,q)=\lim_{n\to\infty}P(\Lambda_n,q)^{1/n}. \tag{1.1}$$

Here Λ_n denotes an n-vertex lattice of type Λ (square, triangular, etc.), with appropriate (e.g., free) boundary conditions. Given the above connection, it is convenient to express our bounds on the ground-state entropy in terms of its exponent $W(\Lambda,q)$. Since nontrivial exact solutions for this function are known in only a very few cases (square lattice for $q=3$ [13], triangular lattice [14], and kagomé lattice for $q=3$ [15]), it is important to exploit and extend general approximate methods that can be applied to all cases. Such methods include rigorous upper and lower bounds, large-q series expansions, and Monte Carlo measurements. Recently, we studied the ground-state entropy in antiferromagnetic Potts models on various lattices and obtained further results with these three methods [16–20].

In the present paper we achieve a substantial generalization of our previous studies. Among other things, we obtain a general rigorous lower bound on the (exponent of the) ground-state entropy that applies for all Archimedean lattices (for definitions, see below) and find further examples of lattices where this lower bound coincides to many orders with a large-q series expansion of the respective W function. This agreement is particularly striking since, *a priori*, a lower bound on a function need not coincide with any, let alone many, of the terms in the series expansion of the function about a given point. We also present calculations of chromatic zeros for a number of lattices and show that they support a conjecture that we have made earlier [20]. The reader is referred to Refs. [16–20] for further background and references.

Although the full set of Archimedean lattices is not as much discussed in the physics literature as the subset of three homopolygonal (i.e., monohedral) ones, viz., square, triangular, and honeycomb, other Archimedean lattices are of both theoretical and experimental interest. For example, the kagomé lattice is of current interest because of the experimental observation of compounds whose behavior can be modeled by quantum Heisenberg antiferromagnets on this

*Electronic address: shrock@insti.physics.sunysb.edu
†Electronic address: tsai@insti.physics.sunysb.edu

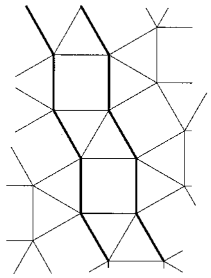

FIG. 1. Section of the $(3^2\cdot 4\cdot 3\cdot 4)$ Archimedean lattice with paths $\mathcal{L}_n$ and $\mathcal{L}_{n'}$ used in the proof of our lower bound indicated with darker lines. See the text for discussion.

lattice, including $SrCr_{8-x}Ga_{4+x}O_{19}$ [SCGO(x)] [21] and, recently, deuteronium jarosite, $[D_3O)Fe_3(SO_4)_2(OD)_6]$ [22]. Related to this, one of the reasons for interest in the kagomé lattice is that on this lattice the quantum Heisenberg antiferromagnet has a disordered ground state with finite entropy and frustration [23]. Indeed, it has been known for a number of years that although the Ising antiferromagnet exhibits ground-state entropy, frustration, and zero long-range order on both the triangular and kagomé lattices, the greater degree of disorder on the kagomé lattice is evidenced by the fact that while the correlation length diverges as $T\to 0$ on the triangular lattice [24], it remains finite on the kagomé lattice [25].

II. SOME GRAPH THEORY BACKGROUND

In this section we include some basic definitions and results in graph theory that will be necessary for our work. A graph (with no loops or multiple bonds) is defined as a collection of vertices and edges (bonds) joining various vertices. In strict mathematical terminology, a graph involves a finite number of vertices; the regular (infinite) lattices that we will consider here are thus limits of graphs, with some appropriate (e.g., free) boundary conditions. The chromatic polynomial $P(G,q)$, defined above, was first introduced by Birkhoff [26] and has been the subject of intensive mathematical study since [27,28,9–12]. The zeros of the chromatic polynomial $P(G,q)$ are denoted the chromatic zeros of G. A graph G that can be colored with q colors, i.e., has $P(G,q)>0$, is said to be q colorable. The chromatic number $\chi(G)$ of a graph G is the minimum (integer) q such that one can color the graph subject to the condition that no two adjacent vertices have the same color, i.e., such that $P(G,q)>0$. The graph G is then said to be $\chi(G)$ chromatic. The graph is uniquely $\chi(G)$ chromatic if and only if $P(G,q=\chi(G))=q!$. A uniquely q-chromatic graph is q partite. These definitions can be extended to the regular infinite lattices of interest here if one defines the latter as the limit as the number of vertices $n\to\infty$ of finite-n lattice graphs with appropriate boundary conditions, such as free boundary conditions. For bipartite lattices one can also use periodic boundary conditions that preserve the bipartite property. Similarly, for a tripartite lattice, one can use periodic boundary conditions that preserve the tripartite property, etc. Henceforth, when we refer to a finite lattice of type Λ, it is understood that appropriate boundary conditions are specified.

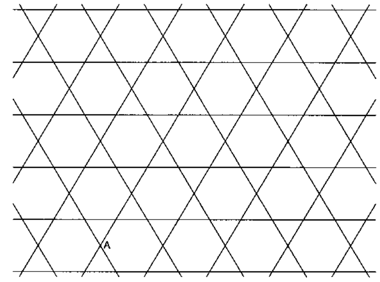

FIG. 2. Section of the $(3\cdot 6\cdot 3\cdot 6)$ Archimedean lattice. The point A labels a vertex that is referred to later in the text.

An Archimedean lattice is defined as a uniform tiling of the plane by regular polygons in which all vertices are equivalent [29]. Such a lattice is specified by the ordered sequence of polygons that one traverses in making a complete circuit around a vertex in a given (say counterclockwise) direction. This is incorporated in the mathematical notation for an Archimedean lattice Λ:

$$\Lambda=\left(\prod_i p_i^{a_i}\right), \tag{2.1}$$

where in the above circuit the notation $p_i^{a_i}$ indicates that the regular polygon p_i occurs contiguously a_i times; it can also occur noncontiguously. Because the starting point is irrelevant, the symbol is invariant under cyclic permutations. For later purposes, when a polygon p_i occurs several times in a noncontiguous manner in the product, we shall denote $a_{i,s}$ as the sum of the a_i's over all of the occurrences of the given p_i in the product. There are eleven Archimedean lattices:

$$\{\Lambda\}=\{(3^6),(4^4),(6^3),(3^4\cdot 6),(3^3\cdot 4^2),(3^2\cdot 4\cdot 3\cdot 4),(3\cdot 4\cdot 6\cdot 4), \tag{2.2}$$

$$(3\cdot 6\cdot 3\cdot 6),(3\cdot 12^2),(4\cdot 6\cdot 12),(4\cdot 8^2)\}. \tag{2.3}$$

Of these lattices, three are homopolygonal, also called monohedral, i.e., they only involve one type of regular polygon: (3^6) (triangular), (4^4) (square), and (6^3) (hexagonal or honeycomb). The other eight are heteropolygonal, i.e., involve tilings with more than one type of regular polygon. The kagomé lattice is $(3\cdot 6\cdot 3\cdot 6)$. Some illustrative pictures of the heteropolygonal lattices are helpful for understanding the results of the present paper. Accordingly, we show in Figs. 1–4 the $(3^2\cdot 4\cdot 3\cdot 4)$, $(3\cdot 6\cdot 3\cdot 6)$ (kagomé), $(3\cdot 12^2)$, and

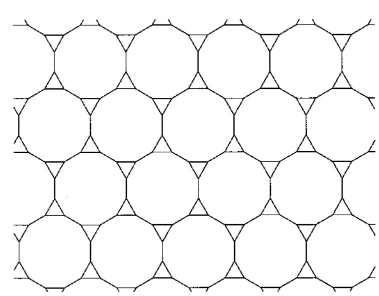

FIG. 3. Section of the $(3\cdot 12^2)$ Archimedean lattice.

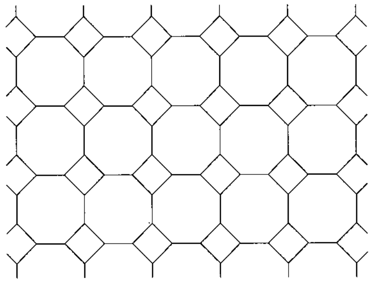

FIG. 4. Section of the $(4\cdot 8^2)$ Archimedean lattice.

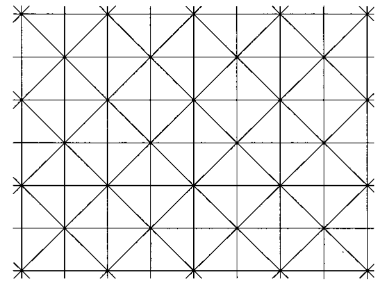

FIG. 5. Section of the $[4\cdot 8^2]$ dual Archimedean (Laves) lattice.

$(4\cdot 8^2)$ lattices. Pictures of others are given in Ref. [29]; see also Ref. [30].

The geometric constraint that the internal angles of each polygon adjacent to a given vertex sum to 2π is

$$\sum_i a_{i,s}\left(1-\frac{2}{p_i}\right)=2. \tag{2.4}$$

The solutions to this equation for integral $a_{i,s}$ and p_i, together with the requirement that a local patch be extendable to tile the plane, yield the Archimedean lattices. The degree Δ of a vertex of a graph G is the number of edges (bonds) that connect to this vertex. For a regular (infinite) lattice, this is the same as the coordination number. For an Archimedean lattice (2.1), the coordination number is

$$\Delta=\sum_i a_{i,s}. \tag{2.5}$$

Of course, for a finite lattice with free boundary conditions, the vertices on the boundary have lower values of Δ than those in the interior; this will not be important for our rigorous bounds, which pertain to the thermodynamic limit on an infinite lattice. For a homopolygonal lattice $\Lambda=(p^a)$, the constraint (2.4) relates the coordination number to p according to

$$\Delta=a=\frac{2p}{p-2} \quad \text{for} \quad \Lambda=(p^a), \tag{2.6}$$

which can also be written in the symmetric form $\Delta^{-1}+p^{-1}=1/2$. The girth $g(G)$ of a graph G is the length of a minimum circuit on the graph. Hence, for an Archimedean lattice (2.1), $g=\min\{p_j\}$. The number of polygons of type p_i per site is given by

$$\nu_{p_i}=\frac{N_{p_i\ per\ v}}{N_{v\ per\ p_i}}=\frac{a_{i,s}}{p_i}. \tag{2.7}$$

The set of homopolygonal Archimedean lattices is invariant under the duality transformation, which interchanges 0-cells (vertices) and 2-cells (faces) and thus maps $(p^a)\to(a^p)$. When one applies the duality transformation to the other eight Archimedean lattices, the resultant lattices are not Archimedean.

The dual of the Archimedean lattice, often called a Laves lattice [29,31], is defined by listing the ordered sequence of vertex types specified by their degrees, $v_i=\Delta_i$, along the boundary of any polygon:

$$\Lambda_{Laves}=\left[\prod_i v_i^{b_i}\right], \tag{2.8}$$

where in the above product the notation $v_i^{b_i}$ indicates that the vertex v_i with degree $v_i=\Delta_i$ occurs contiguously b_i times; it can also occur noncontiguously. As with Archimedean lattices, because the starting point is irrelevant, the symbol is invariant under cyclic permutations. When a vertex of type v_i occurs several times in a noncontiguous manner in the product, we shall denote $b_{i,s}$ as the sum of the b_i's over all of the occurrences of the given v_i in the product. There are eleven dual Archimedean lattices. Just as all vertices are equivalent on an Archimedean lattice, all faces are equivalent on its dual; these are comprised of a single type of polygon p, which, however, does not in general have sides of equal length. Note that

$$p=\sum_i b_{i,s} \tag{2.9}$$

and the girth $g([\Pi_i v_i^{b_i}])=p$. The dual of the Archimedean lattice $(\Pi_i p_i^{a_i})$ is $[\Pi_i v_i^{b_i}]$ with $v_i=p_i$ and $b_i=a_i$. Among Laves lattices, three involve only vertices of one type and are denoted homovertitial and are equivalent to the respective three homopolygonal Archimedean lattices; these are $[3^6]=(6^3)$ (honeycomb), $[4^4]=(4^4)$ (square), and $[6^3]=(3^6)$ (triangular); the other eight are heterovertitial, i.e., involve vertices of at least two types. An example of a heterovertitial Laves lattice is $[4\cdot 8^2]$, the union-jack lattice, shown in Fig. 5.

For these duals of Archimedean lattices, the formula for the number of p-gons per site is

$$\nu_p=\left[\sum_i \frac{b_{i,s}}{v_i}\right]^{-1}. \tag{2.10}$$

Although different vertices on a heterovertitial Laves lattice have different degrees, it will be useful for later purposes to introduce the notion of an effective degree or coordination number, defined by $\Delta_{eff}=\lim_{V\to\infty} 2E/V$, where V and E denote the vertices and edges of the lattice graph. This is given by

$$\Delta_{eff}=\nu_p p. \tag{2.11}$$

This completes our brief review of necessary definitions from graph theory.

TABLE I. Chromatic number $\chi(\Lambda)$ and determination of uniqueness or nonuniqueness of coloring if $q=\chi(\Lambda)$ for the Archimedean lattices. UQC stands for uniquely q-chromatic, and Y and N for yes and no.

Λ	$\chi(\Lambda)$	UQC
(3^6)	3	Y
(4^4)	2	Y
(6^3)	2	Y
$(3^4\cdot 6)$	3	Y
$(3^3\cdot 4^2)$	3	N
$(3^2\cdot 4\cdot 3\cdot 4)$	3	N
$(3\cdot 4\cdot 6\cdot 4)$	3	N
$(3\cdot 6\cdot 3\cdot 6)$	3	N
$(3\cdot 12^2)$	3	N
$(4\cdot 6\cdot 12)$	2	Y
$(4\cdot 8^2)$	2	Y

III. CHROMATIC NUMBERS FOR ARCHIMEDEAN AND DUAL ARCHIMEDEAN LATTICES

As part of our work on ground-state entropy, it has been useful to calculate the chromatic numbers $\chi(\Lambda)$ for the Archimedean lattices and their duals and to determine whether or not these lattices are uniquely q-chromatic for $q=\chi(\Lambda)$. As background, we recall that from the four-color theorem [32], by duality, it follows that $\chi(G)\leqslant 4$ for any planar graph [32]. We find that for all of the nonbipartite Archimedean and dual Archimedean lattices, $\chi=3$ except for the $[3\cdot 12^2]$ Laves lattice, for which $\chi=4$. The latter result follows from the fact that this lattice contains K_4 subgraphs, and $\chi(K_m)=m$. (Here K_m is called the complete graph on m vertices, defined such that each vertex is joined by bonds to every other vertex.) We summarize our results [33] in Tables I and II, together with some properties of these lattices that will be relevant to our calculations of bounds and series.

TABLE II. Chromatic number $\chi(\Lambda)$ and determination of uniqueness or nonuniqueness of coloring if $q=\chi(\Lambda)$ for the heterovertitial duals of Archimedean lattices. UQC stands for uniquely q-chromatic.

Λ	$\chi(\Lambda)$	UQC
$[6^3]$	3	Y
$[4^4]$	2	Y
$[3^6]$	2	Y
$[3^4\cdot 6]$	3	N
$[3^3\cdot 4^2]$	3	N
$[3^2\cdot 4\cdot 3\cdot 4]$	3	N
$[3\cdot 4\cdot 6\cdot 4]$	2	Y
$[3\cdot 6\cdot 3\cdot 6]$	2	Y
$[3\cdot 12^2]$	4	N
$[4\cdot 6\cdot 12]$	3	Y
$[4\cdot 8^2]$	3	Y

IV. A RIGOROUS LOWER BOUND ON $W(\Lambda,q)$ FOR ARCHIMEDEAN Λ

In Refs. [18,19], we derived rigorous lower and upper bounds on $W(\Lambda,q)$ for the triangular and honeycomb lattices, using a coloring matrix method of the type first applied by Biggs to obtain such bounds for the square lattice [34]. We showed that these upper and lower bounds rapidly approached each other for large q and became very restrictive even for moderately large q. Furthermore, we found that for a wide range of q values, the lower bounds were very close to the respective actual values of $W(\Lambda,q)$. Accordingly, here we shall focus on rigorous lower bounds for $W(\Lambda,q)$ for the general class of Archimedean lattices, of which the homopolygonal lattices are a special case. We shall derive a general lower bound applicable to any Archimedean lattice. In addition, we shall derive lower bounds for the duals of Archimedean lattices.

Before proceeding, it is necessary to recall a subtlety in the definition of the function $W(\Lambda,q)$. As we discussed in Ref. [17], the formal equation (1.1) is not, in general, adequate to define $W(\Lambda,q)$ because of a noncommutativity of limits

$$\lim_{n\to\infty}\lim_{q\to q_s} P(\Lambda,q)^{1/n} \neq \lim_{q\to q_s}\lim_{n\to\infty} P(\Lambda,q)^{1/n} \tag{4.1}$$

at certain special points q_s. At these points, one must also specify the order of the limits in Eq. (4.1). We denote these definitions as

$$W(\{G\},q_s)_{D_{qn}} \equiv \lim_{q\to q_s}\lim_{n\to\infty} P(G,q)^{1/n} \tag{4.2}$$

and

$$W(\{G\},q_s)_{D_{nq}} \equiv \lim_{n\to\infty}\lim_{q\to q_s} P(G,q)^{1/n}, \tag{4.3}$$

where $\{G\}$ denotes the $n\to\infty$ limit of the family of n-vertex graphs of type G. One can maintain the analyticity of $W(\{G\},q)$ at the special points q_s of $P(G,q)$ by choosing the order of limits in Eq. (4.2); however, this definition produces a function $W(\{G\},q)_{D_{qn}}$ whose values at the points q_s differ significantly from the values one would get for $P(G,q_s)^{1/n}$ with finite-n graphs G. The definition based on the opposite order of limits (4.3) gives the expected results such as $W(\{G\},q_s)=0$ for $q_s=0,1$ and, for $G\supseteq\triangle$ (i.e., for G containing at least one triangle as a subgraph), also $q_s=2$. However, this second definition yields a function $W(\{G\},q)$ with discontinuities at the set of points $\{q_s\}$. Following Ref. [17], in our results below, in order to avoid having to write special formulas for the points q_s, we shall adopt the definition D_{qn} but at appropriate places will take note of the noncommutativity of limits (4.1). As will be evident from the derivation, our rigorous lower bounds are on the function $W(\Lambda,q)\equiv W(\Lambda,q)_{D_{qn}}$ and they apply for the range of (positive integer) q values for which the relevant coloring matrices (see below) are nontrivial, i.e., for $q\geqslant\chi(\Lambda)$; the values of $\chi(\Lambda)$ were listed in Tables I and II.

Clearly, a general upper bound on a chromatic polynomial for an n-vertex graph G is $P(G,q)\leqslant q^n$. This yields the corresponding upper bound $W(\{G\},q)<q$. Hence, it is natural to define a reduced function that has a finite limit as $q\to\infty$,

$$W_r(\{G\},q)=q^{-1}W(\{G\},q). \tag{4.4}$$

When calculating large-q Taylor series expansions for W functions on regular lattices it is most convenient to carry this out for the related function

$$\overline{W(\Lambda,y)}=\frac{W(\Lambda,q)}{q(1-q^{-1})^{\Delta/2}}, \tag{4.5}$$

for which the large-q series can be written in the form

$$\overline{W(\Lambda,y)}=1+\sum_{m=1}^{\infty} w_{\Lambda,m}y^m, \tag{4.6}$$

with

$$y=\frac{1}{q-1}. \tag{4.7}$$

For duals of Archimedean lattices one can use the same formulas with the replacement $\Delta\to\Delta_{eff}$, where Δ_{eff} was given in Eq. (2.11).

Our rigorous lower bounds are of the form

$$W(\Lambda,q)\geqslant W(\Lambda,q)_{\ell}, \tag{4.8}$$

where the subscript ℓ denotes ''lower,'' and we shall give the explicit expressions for $W(\Lambda,q)_{\ell}$ below. We shall use two other equivalent forms of the bounds, namely, on the functions $W_r(\Lambda,q)$ and $\overline{W(\Lambda,y)}$, both of which have the finite limit $W_r(\Lambda,q=\infty)=\overline{W(\Lambda,y=0)}=1$ and hence are convenient to compare with large-q (small-y) series. Thus, for the latter function, the bounds read

$$\overline{W(\Lambda,y)}\geqslant\overline{W(\Lambda,y)}_{\ell}, \tag{4.9}$$

where the reduced lower bound function is defined by analogy with Eq. (4.5) as

$$\overline{W(\Lambda,y)}_{\ell}=\frac{W(\Lambda,q)_{\ell}}{q(1-q^{-1})^{\Delta/2}}. \tag{4.10}$$

Our general rigorous lower bound, which is a major result of the present paper, is proved in the following theorem.

Theorem. Let $\Lambda=(\prod_i p_i^{a_i})$ be an Archimedean lattice. Then for (integer) $q\geqslant\chi(\Lambda)$, $W(\Lambda,q)\equiv W(\Lambda,q)_{D_{qn}}$ has the lower bound

$$W\left(\left(\prod_i p_i^{a_i}\right),q\right)_{\ell}=\frac{\prod_i D_{p_i}(q)^{\nu_{p_i}}}{q-1}, \tag{4.11}$$

where the $\{i\}$ in the product label the set of p_i-gons involved in Λ, ν_{p_i} was defined in Eq. (2.7), and

$$D_k(q)=\frac{P(C_k,q)}{q(q-1)}=\sum_{s=0}^{k-2}(-1)^s\binom{k-1}{s}q^{k-2-s}, \tag{4.12}$$

where $P(C_k,q)=(q-1)^k+(-1)^k(q-1)$ is the chromatic polynomial for a k-vertex circuit graph, i.e., polygon. This lower bound takes a somewhat simpler form in terms of the related function $\overline{W(\Lambda,y)}_{\ell}$:

$$\overline{W\left(\left(\prod_i p_i^{a_i}\right),y\right)}_{\ell}=\prod_i [1+(-1)^{p_i}y^{p_i-1}]^{\nu_{p_i}}. \tag{4.13}$$

Proof. We consider a sequence of finite two-dimensional Archimedean lattices with periodic boundary conditions in one direction, say the x direction, and either periodic or free boundary conditions in the orthogonal, y, direction. Denote the lengths of the finite lattice in these two directions as m and n and the finite lattice of type Λ as $\Lambda_{m\times n}$. Extending the method that Biggs used for the square lattice [34], we introduce a coloring matrix T, somewhat analogous to the transfer matrix for statistical mechanical spin models. The construction of T begins by considering an n-vertex path $\mathcal{L}_n$ along a vertical path on $\Lambda_{m\times n}$. For the square lattice, it is obvious what is meant here, and one can also represent the other homopolygonal lattices as square lattices with bonds added or deleted (for the triangular and honeycomb lattices, respectively; see Fig. 1 of Ref. [18] and the discussion in Ref. [19]). Thus, as is well known, the triangular lattice can be deformed so that it is represented as a square lattice with bonds added to connect the lower left and upper right vertices of each square, and the honeycomb lattice can be deformed to make a brick lattice, with the long side of the bricks oriented vertically. These deformations do not affect the coloring properties of the lattices. With these representations of the triangular and honeycomb lattices, one can choose a vertical path in the same manner as for the square lattice. Analogous paths can be defined on heteropolygonal Archimedean lattices [an illustration is given in Fig. 1 for the $(3^2\cdot4\cdot3\cdot4)$ lattice]. In all cases except the $(4\cdot6\cdot12)$ lattice, these are simple (i.e., unbranched) chains. For the $(4\cdot6\cdot12)$ lattice, the paths are chains with single-bond branches. We shall give the proof first for the seven Archimedean lattices where the paths are simple chains that do not intersect, namely, the three homopolygonal lattices and the $(3^2\cdot4^2)$, $(3^2\cdot4\cdot3\cdot4)$, $(3\cdot4\cdot6\cdot4)$, and $(4\cdot8^2)$ heteropolygonal lattices. We then give the proof for the three remaining lattices where the paths do intersect and, separately, for the special case of the $(4\cdot6\cdot12)$ lattice, where the paths, although nonintersecting, are branched chains. The number of allowed colorings of the path $\mathcal{L}_n$ is $P(\mathcal{L}_n,q)=q(q-1)^{n-1}\equiv\mathcal{N}$. Now focus on two adjacent paths $\mathcal{L}_n$ and $\mathcal{L}_{n'}$. Define compatible q colorings of these paths as colorings such that no two vertices $v\in\mathcal{L}_n$ and $v'\in\mathcal{L}_n'$ connected by a bond of $\Lambda_{m\times n}$ have the same color. One can then associate with this pair of paths an $\mathcal{N}\times\mathcal{N}$ dimensional symmetric matrix T with entries $T_{\mathcal{L}_n,\mathcal{L}_n'}=1$ or 0 if the q colorings of $\mathcal{L}_n$ and $\mathcal{L}_n'$ are or are not compatible, respectively. Then for fixed lengths of the lattice in the x and y directions, m and n, $P(\Lambda_{m\times n},q)=\mathrm{Tr}(T^m)$. For a given n, since T is a nonnegative matrix, one can apply the Perron-Frobenius theorem

[35] to conclude that T has a real positive eigenvalue $\lambda_{max,n}(q)$. Hence, for fixed n,

$$\lim_{m\to\infty} \mathrm{Tr}(T^m)^{1/(mn)} \to \lambda_{max}^{1/n} \tag{4.14}$$

so that

$$W(\Lambda,q)=\lim_{n\to\infty}\lambda_{max}^{1/n}. \tag{4.15}$$

Denote the column sum $\kappa_j(T)=\Sigma_{i=1}^{\mathcal{N}}T_{ij}$ [equal to the row sum $\rho_j(T)=\Sigma_{i=1}^{\mathcal{N}}T_{ji}$ since $T^T=T$] and $S(T)=\Sigma_{i,j=1}^{\mathcal{N}}T_{ij}$; note that $S(T)/\mathcal{N}$ is the average row (column) sum. The lower bound is then a consequence of the ($r=1$ special case of the) theorem that for a nonnegative symmetric matrix T [36] $\lambda_{max}(T)\geqslant[S(T^r)/\mathcal{N}]^{1/r}$ for $r=1,2,\ldots$ together with Eq. (4.15):

$$W(\Lambda,q)\geqslant W(\Lambda,q)_{\ell}=\lim_{n\to\infty}\left(\frac{S(T)}{\mathcal{N}}\right)^{1/n}. \tag{4.16}$$

This is the general method; we next proceed to calculate $S(T)$. To do this we observe that the adjacent paths $\mathcal{L}_n$ and $\mathcal{L}_n'$ can be chosen such that the striplike section of the lattice between them contains each of the types of polygons comprising Λ (this essentially amounts to the orientation of the lattice to define the vertical direction). Each polygon p_i has the chromatic polynomial given above as $P(C_{p_i},q)$. Next, we use a basic theorem from graph theory: If G and G' are graphs that intersect in a complete graph K_r [37], then $P(G\cup G',q)=P(G,q)P(G',q)/P(K_r,q)$, where $P(K_r,q)=\Pi_{s=0}^{r-1}(q-s)$. We then apply this theorem, taking into account that the number of polygons of type p_i per vertex is ν_{p_i}, to obtain the result that for paths of length n, $S(T)=c(q)\Pi_i D_{p_i}(q)^{\nu_{p_i}(n+b)}$, where b is an unimportant constant independent of n, and the prefactor $c(q)=q(q-1)(q-2)$ if Λ contains triangles, $\Lambda\supseteq\triangle$, and $c(q)=q(q-1)$ otherwise. Then taking the $n\to\infty$ limit in Eq. (4.16) yields Eq. (4.11). Equivalently, using the definition of the reduced function (4.5), we obtain Eq. (4.13). For the three lattices, viz., $(3^4\cdot 6)$, $(3\cdot 6\cdot 3\cdot 6)$, and $(3\cdot 12^2)$, where the adjacent paths $\mathcal{L}_n$ and $\mathcal{L}_n'$ do intersect, the calculation involves a technical complication due to these intersections: The expression for $S(T)$ involves an additional factor of $(q-1)^{\lambda n}$, where λ is the fraction of points on each path $\mathcal{L}_n$ that coincide with points on $\mathcal{L}_n'$, but this factor is exactly canceled by the same additional factor in the expression for $\mathcal{N}$ in the denominator of the ratio $S(T)/\mathcal{N}$. The additional factor in the denominator arises because one must correct for the undercounting of the points on the paths $\mathcal{L}_n$ due to the intersections. Because the factor cancels, the result is the same as for the lattices with nonintersecting adjacent paths $\mathcal{L}_n$ and $\mathcal{L}_n'$.

Finally, we consider the $(4\cdot 6\cdot 12)$ lattice. Let us consider the lattice as oriented so that the 12-gons have vertical left and right bonds and horizontal top and bottom bonds, with a hexagon vertically above the 12-gon and adjacent to it, and label the vertices of each 12-gon in a clockwise manner starting with the left vertex on the top bond. The path $\mathcal{L}_n$ that we use goes from vertex 6 of a given 12-gon to vertices 5,4,3 and then crosses over to vertex 8 of the adjacent 12-gon in the upper right (‘‘northeast’’) direction, has a one-bond branch to vertex 7 of this 12-gon, and then continues along on vertices 8–12 and then 1, with a one-bond branch to vertex 2, continuing from vertex 1 upward to vertex 6 of the vertically adjacent 12-gon in the northwest direction, and so forth. The strip enclosed by two adjacent paths of length n of this type has a chromatic polynomial

$$S(T)=q(q-1)[D_4(q)^3D_6(q)^2D_{12}(q)+2D_3(q)D_4(q)^2D_6(q)+qD_3(q)^2D_4(q)]^{n/12}. \tag{4.17}$$

The chromatic polynomial for the path of length n is the same as that for an unbranched path, since both are tree graphs. Hence, for this case, the lower bound actually reads $W((4\cdot 6\cdot 12),q)\geqslant W((4\cdot 6\cdot 12),q)_{\ell'}$, where

$$W((4\cdot 6\cdot 12),q)_{\ell'}=\frac{[D_4(q)^3D_6(q)^2D_{12}(q)+2D_3(q)D_4(q)^2D_6(q)+qD_3(q)^2D_4(q)]^{1/12}}{q-1}. \tag{4.18}$$

For the above-mentioned range of q under consideration here, i.e., $q\geqslant\chi((4\cdot 6\cdot 12))=2$, the two additional terms in the square brackets are positive, so that

$$W((4\cdot 6\cdot 12),q)_{\ell}=\frac{D_4(q)^{1/4}D_6(q)^{1/6}D_{12}(q)^{1/12}}{q-1}, \tag{4.19}$$

which is of the form (4.11). [As we shall discuss below, the difference between the bounds (4.18) and (4.19) is very small.] This completes the proof.

For the homopolygonal Archimedean lattices $\Lambda=(p^a)$ [with $a=\Delta$ given by Eq. (2.5) and $\nu_p=2/(p-2)$ by Eq. (2.7)], our bound (4.11) reduces to

$$W((p^\Delta),q)_{\ell}=\frac{D_p(q)^{2/(p-2)}}{q-1} \tag{4.20}$$

or equivalently, Eq. (4.13) reduces to

$$\overline{W}((p^\Delta),y)_{\ell}=[1+(-1)^p y^{p-1}]^{2/(p-2)}. \tag{4.21}$$

In Table III we list the explicit forms of the lower bounds

TABLE III. Rigorous lower bounds $\overline{W(\Lambda,y)}_{\ell}$ for Archimedean lattices $\Lambda=(\Pi_i p_i^{a_i})$ given by Eq. (4.13). For homopolygonal Archimedean lattices $\Lambda=(p^{\Delta})$, the Taylor series expansion of $\overline{W(\Lambda,y)}_{\ell}$ coincides to $O(y^{i_c})$ with the series expansion of $\overline{W(\Lambda,y)}$, where $i_c=i_{max}=2(p-1)$, the values of which are listed in the third column, and the subscript c stands for ''coinciding.'' For other lattices, the series expansions of $\overline{W(\Lambda,y)}_{\ell}$ and $\overline{W(\Lambda,y)}$ coincide to at least $O(y^{i_c})$.

Λ	$\overline{W(\Lambda,y)}_{\ell}$	i_c
(3^6)	$(1-y^2)^2$	4
(4^4)	$1+y^3$	6
(6^3)	$(1+y^5)^{1/2}$	10
$(3^4\cdot 6)$	$(1-y^2)^{4/3}(1+y^5)^{1/6}$	4
$(3^3\cdot 4^2)$	$(1-y^2)(1+y^3)^{1/2}$	4
$(3^2\cdot 4\cdot 3\cdot 4)$	$(1-y^2)(1+y^3)^{1/2}$	4
$(3\cdot 6\cdot 3\cdot 6)$	$(1-y^2)^{2/3}(1+y^5)^{1/3}$	8
$(3\cdot 4\cdot 6\cdot 4)$	$(1-y^2)^{1/3}(1+y^3)^{1/2}(1+y^5)^{1/6}$	5
$(3\cdot 12^2)$	$(1-y^2)^{1/3}(1+y^{11})^{1/6}$	13
$(4\cdot 6\cdot 12)$	$(1+y^3)^{1/4}(1+y^5)^{1/6}(1+y^{11})^{1/12}$	11
$(4\cdot 8^2)$	$(1+y^3)^{1/4}(1+y^7)^{1/4}$	12

$\overline{W(\Lambda,y)}_{\ell}$ for the Archimedean lattices, including a comparison with small-y series, to be discussed below.

We give some illustrations of the method of the proof here. First, we illustrate this for a lattice where the paths $\mathcal{L}_n$ do not intersect, namely, the $(3^2\cdot 4\cdot 3\cdot 4)$ lattice shown in Fig. 1. The paths $\mathcal{L}_n$ and $\mathcal{L}_n'$ are depicted by the thicker lines, and the strip between these consists of a sequence of squares and double triangles. For technical convenience, we consider a path to start at the lower left-hand vertex of a square and we take n to be odd so that the path length is even. The sum $S(T)$ is calculated starting from the basic graph G_{433} comprised of a square and two adjacent triangles (say above the square) for which the chromatic polynomial is $P(G_{433},q)=q(q-1)D_3(q)^2D_4(q)$. For a strip lying between the adjacent paths $\mathcal{L}_n$ and $\mathcal{L}_n'$ (both of length $n-1$), starting the count from the lower left corner of a square, there are $r=(n-1)/2$ G_{433} graphs, so, in an obvious notation,

$$S(T)=P(G_{433}^r,q)=q(q-1)[D_3(q)^2D_4(q)]^{(n-1)/2}. \tag{4.22}$$

Dividing by $\mathcal{N}=q(q-1)^{n-1}$ and taking the $n\to\infty$ limit of the $(1/n)$th power of the ratio as in Eq. (4.16), one obtains the rigorous lower bound

$$W((3^2\cdot 4\cdot 3\cdot 4),q)_{\ell}=\frac{D_3(q)D_4(q)^{1/2}}{q-1}, \tag{4.23}$$

which is seen to be the special case of Eq. (4.11) for this lattice. Another explicit example is provided by the $(4\cdot 8^2)$ lattice, which we have previously discussed [19].

To illustrate the proof in a case where the paths $\mathcal{L}_n$ and $\mathcal{L}_n'$ have a nonzero overlap, we discuss the $(3\cdot 6\cdot 3\cdot 6)$ lattice, shown in Fig. 2. To visualize the path $\mathcal{L}_n'$, start at the vertex A at which two triangles touch and move ''northwest'' to the leftmost vertex of the hexagon above these triangles; then move northeast to the vertex common to the two triangles above the hexagon, then northwest again to the leftmost vertex of the next higher hexagon, etc., continuing upward in this zigzag manner. For $\mathcal{L}_n'$, start from the same vertex, but move first northeast to the rightmost vertex of the hexagon above the triangles, then northwest to the vertex common to the two triangles above the hexagon, and so forth. For technical convenience, we consider the paths to be of length a multiple of 4. Evidently, the n-vertex paths $\mathcal{L}_n$ and $\mathcal{L}_n'$ so defined have a nonzero overlap (intersection) consisting of the vertices that are shared in common by the pairs of triangles traversed along the route. For consistency, we assign alternate intersection points to be on adjacent paths. These intersection points comprise 1/3 of the total number n of the vertices along each path. The strip between the paths $\mathcal{L}_n$ and $\mathcal{L}_n'$ consists of a sequence of triangle-hexagon-triangle graphs, which we denote as G_{363}. For a path $\mathcal{L}_n$ starting from a vertex of type A, there are $r=(n-1)/3$ linked G_{363} graphs in this strip. The chromatic polynomial of the strip is

$$S(T)=P(G_{363}^r,q)=q[(q-1)D_3(q)^2D_6(q)]^{(n-1)/3}. \tag{4.24}$$

However, in evaluating the denominator for Eq. (4.16), it is necessary to correct for the vertices that are common to both paths; taking into account that these comprise a third of the total points on each path and including this correction factor yields the denominator $\mathcal{N}=q(q-1)^{4n/3}$. Evaluating Eq. (4.16) then gives the resulting lower bound

$$W((3\cdot 6\cdot 3\cdot 6)_{\ell})=\frac{D_3(q)^{2/3}D_6(q)^{1/3}}{q-1}, \tag{4.25}$$

which again is the special case of Eq. (4.11) for this lattice.

Finally, we discuss the difference between the lower bounds (4.18) and (4.19) for the $(4\cdot 6\cdot 12)$ lattice. This difference shows that, at least for this lattice, the special case (4.19) is not an optimal lower bound. However, the numerical difference is extremely small. At $q=\chi((4\cdot 6\cdot 12))=2$, the bounds (4.18) and (4.19) are identical and equal to 1, which is also the exact value of $W((4\cdot 6\cdot 12),q=2)_{D_{nq}}$ [see Eq. (4.33) below]. At $q=3$, the difference between the bounds (4.18) and (4.19) is 1.3×10^{-5}; this difference decreases monotonically for larger q. This reflects the fact that the large-q series expansions of the corresponding reduced lower bound functions are identical to $O(q^{-14})$:

$$W_r((4\cdot 6\cdot 12),q)_{\ell'}-W_r((4\cdot 6\cdot 12),q)_{\ell}=\frac{1}{6}q^{-15}+O(q^{-16}). \tag{4.26}$$

We comment on some general properties of our rigorous lower bound on $W(\Lambda,q)$ in Eq. (4.11) and the consequent bound on the related functions $W_r(\Lambda,q)$ and $\overline{W(\Lambda,y)}$ for Archimedean lattices Λ. First,

$$W\left(\left(\prod_i p_i^{a_i}\right),q\right)_{\ell}\sim\frac{q^{\sum_i \nu_i(p_i-2)}}{q}\sim q \quad \text{as} \quad q\to\infty, \tag{4.27}$$

where $\Sigma_i \nu_i(p_i - 2) = 2$ as a consequence of eq. (2.4). Hence, $\lim_{q\to\infty} W_r((\Pi_i p_i^{a_i}),q)_\ell = 1$.

Second, note that when we compare our lower bound on $W_r(\Lambda,q)$ to the large-q Taylor series expansion on each lattice Λ, this comparison is obviously restricted to the range of q for which these series expansions are applicable. As we discussed in Ref. [17], for a given graph G, when one generalizes q to a complex variable, the reduced function $W_r(\{G\},q) = q^{-1}W(\{G\},q)$ is analytic in the q plane except on the union of boundaries $\mathcal{B}$. These boundaries can separate the q plane into various regions R_i such that one cannot analytically continue $W(\{G\},q)$ from one region to another. We defined the region containing the positive real q axis from a minimal value $q_c(\Lambda)$ to $q=\infty$ as R_1. Clearly, the large-q Taylor series for $W_r(\{G\},q)$ apply in this region. Here, $q_c(G)$ is thus defined as the maximal (finite) real value of q where $W(\{G\},q)$ is nonanalytic. All of these considerations apply for the case of regular lattice graphs Λ defined, as above, as the $n\to\infty$ limit of finite Λ_n lattices. As our general study and explicit exact solutions in Ref. [17] showed for $q \in R_1$, the limits (4.1) commute and hence the two definitions (4.2) and (4.3) coincide. Hence, in our discussions of series, we shall not need to distinguish between these two different definitions of $W(\Lambda,q)$. Furthermore, in this region R_1, just as one can extend the definition of the function $W(\Lambda,q)$ from integer to real q, so also one can carry out the same extension of the lower bound $W(\Lambda,q)_\ell$. Hence, for $q \geq q_c(\Lambda)$, the lower bound (4.11) applies for real and not just integer q. In general,

$$\chi(\Lambda) \leq q_c(\Lambda). \tag{4.28}$$

In Refs. [16] and [17], we showed that $q_c((3^6)) = 4$, $q_c((4^4)) = 3$, and $q_c((6^3)) = (3+\sqrt{5})/2$.

Third, $W(\Lambda,q)_\ell$ is a monotonically increasing function of real q for $q \geq \chi(\Lambda)$ [38].

Fourth, if two different lattices involve the same set of polygons and have the property that each type of polygon p_i occurs an equal total number of times as one makes the circuit around each vertex, then our lower bound (4.11) is the same for both. This is true of the $(3^3\cdot 4^2)$ and $(3^2\cdot 4\cdot 3\cdot 4)$ lattices, for which the lower bound is given by Eq. (4.23).

Fifth, it should be remarked that one can often choose different types of paths $\mathcal{L}_n$ and $\mathcal{L}'_n$. For example, in Ref. [18] we derived a lower bound $W((6^3),q)_{\ell,dimer} = (q-1)^{3/2}/q^{1/2}$ by choosing paths consisting of certain dimers. In Ref. [19], using paths of the type described here, we obtained the lower bound of the form (4.11),

$$W((6^3),q)_\ell = \frac{D_6(q)^{1/2}}{q-1} \geq W((6^3),q)_{\ell,dimer}, \tag{4.29}$$

which, as indicated, is slightly more stringent.

Finally, the fact that for the circuit with an even number, say $2k$, of vertices the chromatic polynomial is $P(C_{2k},q=2)=2$, together with the definition (4.12), it follows that [39]

$$D_{2k}(q=2) = 1. \tag{4.30}$$

Hence, for bipartite Archimedean lattices Λ_{bip}, where our lower bound (4.11) can be applied at $q = \chi(\Lambda_{bip}) = 2$, we have

$$W(\Lambda_{bip}, q=2)_\ell = 1. \tag{4.31}$$

Thus, in this case, although our bound refers to $W(\Lambda,q)_{D_{qn}}$, it has the same value as $W(\Lambda_{bip},q=2)_{D_{nq}}$, as given below in Eq. (4.33).

Note that for lattices Λ_{UQC} that are uniquely q chromatic (UQC) for $q=\chi(\Lambda)$, it follows, *a fortiori*, that

$$W(\Lambda_{UQC}, q=\chi(\Lambda))_{D_{nq}} = 1. \tag{4.32}$$

Thus, in particular, for a bipartite lattice

$$W(\Lambda_{bip}, q=2)_{D_{nq}} = 1 \tag{4.33}$$

and for the tripartite lattices $(3^6) = [6^3]$, $(3^4\cdot 6)$, $[4\cdot 8^2]$, and $[4\cdot 6\cdot 12]$,

$$W(\Lambda_{trip}, q=3)_{D_{nq}} = 1. \tag{4.34}$$

V. A RIGOROUS LOWER BOUND ON $W(\Lambda,q)$ FOR DUAL ARCHIMEDEAN Λ

Using methods similar to those that we used for the Archimedean lattices, we have also calculated rigorous lower bounds for the duals of these lattices. As with the lower bounds for Archimedean lattices, our bounds for the dual lattices again apply for $q \geq \chi(\Lambda)$ for each Λ. For seven of the lattices, we are able to obtain the respective lower bounds by using paths $\mathcal{L}_n$ that either do not intersect, in the case of the homovertitial lattices and also for $[3^4\cdot 6]$, $[3^3\cdot 4^2]$, $[3^2\cdot 4\cdot 3\cdot 4]$, and $[3\cdot 4\cdot 6\cdot 4]$, or intersect, in the case of the $[3\cdot 6\cdot 3\cdot 6]$ lattice. For these, by the same methods as before, we obtain the general rigorous lower bound

$$W\left(\left[\prod_i v_i^{b_i}\right],q\right)_\ell = \frac{D_p(q)^{\nu_p}}{q-1}, \tag{5.1}$$

where p and ν_p were given in Eqs. (2.9) and (2.10). Using Eq. (4.10) with Δ replaced by Δ_{eff} given in Eq. (2.11), this is equivalent to

$$\overline{W}\left(\left[\prod_i v_i^{b_i}\right],q\right)_\ell = [1+(-1)^p y^{p-1})^{\nu_p}]. \tag{5.2}$$

The proof is the same as the one given before for Archimedean lattices, with the simplification that only one kind of polygon is involved in the calculation of $S(T)$. The homovertitial Laves lattices have already been dealt with as homopolygonal Archimedean lattices; for the heterovertitial Laves lattices satisfying the above condition on paths we find the specific bounds

$$\begin{aligned} W([3^4\cdot 6],q)_\ell &= W([3^3\cdot 4^2],q)_\ell \\ &= W([3^2\cdot 4\cdot 3\cdot 4],q)_\ell \\ &= \frac{D_5(q)^{2/3}}{q-1} \end{aligned} \tag{5.3}$$

and

$$W([3\cdot6\cdot3\cdot6],q)_{\ell}=W([3\cdot4\cdot6\cdot4],q)_{\ell} = \frac{D_4(q)}{q-1} = \frac{(q^2-3q+3)}{q-1}, \quad (5.4)$$

$$W([4\cdot8^2],q)_{\ell,\mathcal{L}} = \frac{D_3(q)^2}{q-1} = \frac{(q-2)^2}{q-1}. \quad (5.5)$$

We note that the lower bound (5.4) is the same as the one that we derived for the square lattice $(4^4)=[4^4]$ and the lower bound (5.5) is the same as the one that we derived for the triangular lattice $(3^6)=[6^3]$.

However, for one of the lattices, viz., $[4\cdot8^2]$, where such paths exist, we have been able to obtain a more stringent lower bound by using a different kind of coloring matrix method, in which this matrix is defined in terms of the compatibility not of adjacent paths, but of adjacent chains of graphs that are more complicated than paths. Consider the $[4\cdot8^2]$ lattice shown in Fig. 5. For this lattice, one obtains the lower bound (5.5). But rather than paths, one can consider chains of graphs constructed as follows. Consider a vertical line on the lattice and let $\mathcal{M}_n$ denote the chain of triangles whose bases include vertices from 1 to n along this vertical line and whose apexes point to the right. Evidently, each pair of sequential triangles intersect at the common vertex on their bases. Define $\mathcal{M}'_n$ to be the corresponding equal-length chain of triangles whose bases form the unit segments along the next (adjacent) vertical line of the lattice to the immediate right of the previous one. For technical convenience, let n be odd. Then define a new type of (symmetric) coloring matrix, of dimension $\mathcal{N}\times\mathcal{N}$, where $\mathcal{N}=P(\mathcal{M}_n,q)=P(\mathcal{M}'_n,q)$, with entries $T_{\mathcal{M}_n,\mathcal{M}'_n}=1$ or 0 if the q colorings of the chains of graphs $\mathcal{M}_n$ and $\mathcal{M}'_n$ are or are not compatible, respectively. One then proceeds as before to derive the lower bound (4.16). In the present case,

$$P(\mathcal{M}_n,q)=q[(q-1)(q-2)]^r, \quad r=\frac{n-1}{2} \quad (5.6)$$

and

$$S(T)=q(q-1)[(q-2)^2(q^2-5q+7)]^r, \quad r=\frac{n-1}{2} \quad (5.7)$$

so that, evaluating the limit in Eq. (4.16), we obtain

$$W([4\cdot8^2],q)_{\ell}=\left[\frac{(q-2)(q^2-5q+7)}{(q-1)}\right]^{1/2}. \quad (5.8)$$

For the relevant range, $q\geq\chi([4\cdot8^2])=3$, the lower bound (5.8) always lies above Eq. (5.5), i.e., is more stringent. We list the corresponding lower bound $\overline{W}([4\cdot8^2],y)_{\ell}$ in Table IV). Using this different coloring matrix method based on chains of graphs that are not simple paths, we similarly obtain the following rigorous lower bounds for the other two dual Archimedean lattices:

TABLE IV. Rigorous lower bounds $\overline{W}(\Lambda,y)_{\ell}$ for duals of Archimedean lattices $\Lambda=[\Pi_i v_i^{b_i}]$, where $v_i=\Delta_i$. For homovertitial duals $\Lambda=[v^b]=[\Delta^p]$, where p and Δ are related by Eq. (2.6), the Taylor series expansion of $\overline{W}(\Lambda,y)_{\ell}$ coincides to $O(y^{i_c})$ with the series expansion of $\overline{W}(\Lambda,y)$, where $i_c=i_{max}=2(p-1)$, the values of which are listed in the third column, and the subscript c stands for coinciding. For other lattices, the series expansions of $\overline{W}(\Lambda,y)_{\ell}$ and $\overline{W}(\Lambda,y)$ coincide to at least $O(y^{i_c})$.

Λ	$\overline{W}(\Lambda,y)_{\ell}$	i_c
$[3^6]$	$(1+y^5)^{1/2}$	10
$[4^4]$	$1+y^3$	6
$[6^3]$	$(1-y^2)^2$	4
$[3^4\cdot6]$	$(1-y^4)^{2/3}$	7
$[3^3\cdot4^2]$	$(1-y^4)^{2/3}$	7
$[3^2\cdot4\cdot3\cdot4]$	$(1-y^4)^{2/3}$	7
$[3\cdot6\cdot3\cdot6]$	$1+y^3$	4
$[3\cdot4\cdot6\cdot4]$	$1+y^3$	4
$[3\cdot12^2]$	$(1+y)^2(1-3y+2y^2)^{2/3}$	3
$[4\cdot6\cdot12]$	$(1+y)^2(1-y)(1-3y+3y^2)^{1/3}$	3
$[4\cdot8^2]$	$(1+y)^2(1-y)^{1/2}(1-3y+3y^2)^{1/2}$	3

$$W([3\cdot12^2],q)_{\ell}=\frac{[(q-2)(q-3)]^{2/3}}{(q-1)^{1/3}}, \quad (5.9)$$

$$W([4\cdot6\cdot12],q)_{\ell}=\frac{(q-2)(q^2-5q+7)^{1/3}}{(q-1)^{2/3}}. \quad (5.10)$$

The corresponding lower bounds $\overline{W}(\Lambda,y)_{\ell}$ are listed in Table IV. To retain the symmetry between the Archimedean and Laves lattices, we also list the lower bounds for the square, triangular, and honeycomb lattice in their respective Laves forms $[4^4]$, $[6^3]$, and $[3^6]$.

VI. LARGE-q SERIES

A priori, a lower bound on a given function need not agree with any, let alone many, terms in the Taylor series expansion of that function about some special point. In our earlier comparison of rigorous lower bounds on $\overline{W}(\Lambda,y)$ with large-q (i.e., small-y) series expansions for the respective exact $\overline{W}(\Lambda,y)$ functions for the homopolygonal lattices $\Lambda=(p^\Delta)$, where $\Delta=2p/(p-2)$, we found [17–19] that our lower bounds and the series coincided to $O(y^{i_c})$, where

$$i_c=i_{max}=2(p-1). \quad (6.1)$$

In the case of the (6^3) (honeycomb) lattice, our lower bound thus coincided with the small-y series for the exact function to $O(y^{10})$, i.e., the first eleven terms. Thus, in addition to being a rigorous lower bound, our expression for $\overline{W}((6^3),y)$ became an extremely accurate approximation to the exact function, $\overline{W}((6^3),y)$ for even moderately large q. We also considered one heteropolygonal Archimedean lattice, the $(4\cdot8^2)$ lattice, and calculated both a lower bound and small-

y series for $\overline{W}((4\cdot 8^2),y)$ [19]; in this case we found that our lower bound coincided with the first thirteen terms of our series.

Here we report our calculations of small-y series for $\overline{W}(\Lambda,y)$ on the remaining seven Archimedean lattices and compare these with our rigorous lower bounds, thereby achieving a complete comparison for all Archimedean lattices. Our calculations use the methods of Ref. [40]. Since our main purpose was an exploratory study of the extent to which our lower bounds coincided with the series expansions, we have not attempted to compute the latter to very high order; it is straightforward to carry these expansions to higher order (e.g., [41]).

Our results are listed below:

$$\overline{W}((3^4\cdot 6),y)=1-\frac{4}{3}y^2+\frac{2}{9}y^4+O(y^5), \qquad (6.2)$$

$$\overline{W}((3^3\cdot 4^2),y)=\overline{W}((3^2\cdot 4\cdot 3\cdot 4),y) =1-y^2+\frac{y^3}{2}+0y^4+O(y^5), \qquad (6.3)$$

$$\overline{W}((3\cdot 4\cdot 6\cdot 4),y)=1-\frac{y^2}{3}+\frac{y^3}{2}-\frac{y^4}{9}+0y^5+O(y^6), \qquad (6.4)$$

$$\overline{W}((3\cdot 6\cdot 3\cdot 6),y)=1-\frac{2}{3}y^2-\frac{1}{9}y^4+\frac{1}{3}y^5-\frac{4}{3^4}y^6-\frac{2}{9}y^7 -\frac{7}{3^5}y^8+O(y^9), \qquad (6.5)$$

$$\overline{W}((3\cdot 12^2),y)=1-\frac{1}{3}y^2-\frac{1}{9}y^4-\frac{5}{3^4}y^6-\frac{10}{3^5}y^8-\frac{22}{3^6}y^{10} +\frac{1}{6}y^{11}-\frac{154}{3^8}y^{12}-\frac{1}{18}y^{13}+O(y^{14}), \qquad (6.6)$$

$$\overline{W}((4\cdot 6\cdot 12),y)=1+\frac{1}{4}y^3+\frac{1}{6}y^5-\frac{3}{32}y^6+\frac{1}{24}y^8+\frac{7}{128}y^9 -\frac{5}{72}y^{10}+\frac{13}{192}y^{11}+O(y^{12}), \qquad (6.7)$$

$$\overline{W}((4\cdot 8^2),y)=1+\frac{1}{4}y^3-\frac{3}{2^5}y^6+\frac{1}{4}y^7+\frac{7}{2^7}y^9+\frac{1}{2^4}y^{10} -\frac{77}{2^{11}}y^{12}+O(y^{13}). \qquad (6.8)$$

We have also calculated low-order series for dual Archimedean lattices in order to make an initial comparison with our rigorous lower bounds. We have compared each of these series with the corresponding small-y Taylor series expansions of our rigorous lower bounds in Tables III and IV.

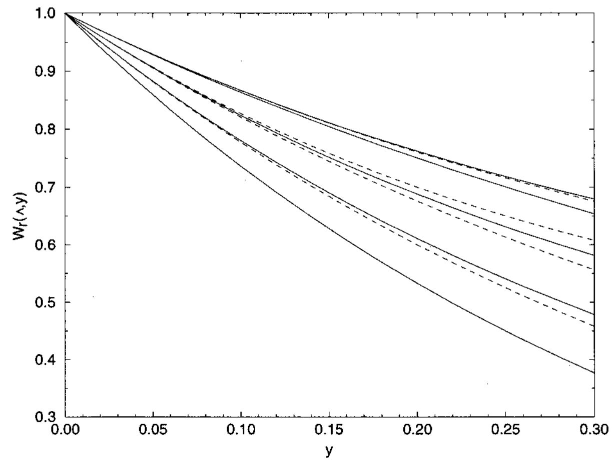

FIG. 6. Plots of $W_r(\Lambda,y)=q^{-1}W(\Lambda,y)$ as a function of $y=1/(q-1)$ for Archimedean lattices Λ. For visual clarity, the curves are shown alternately as solid (s) and dashed (d). The order of the curves, from bottom to top, is (3^6) (s), $(3^4\cdot 6)$ (d), $(3^3\cdot 4^2)$ (s), $(3\cdot 6\cdot 3\cdot 6)$ (d), $(3\cdot 4\cdot 6\cdot 4)$ (s), (4^4) (d), $(3\cdot 12^2)$ (s), (6^3) (d), and $(4\cdot 8^2)$ and $(4\cdot 6\cdot 12)$ as a single solid curve to this resolution. See the text for further details.

We find that the latter expansions coincide at least to $O(y^{i_c})$, where the respective values of i_c are listed in Table III for each lattice. As is evident from this table, the striking fact that we showed previously [18,19], viz., that the series expansions for $\overline{W}(\Lambda,y)_\ell$ coincide to very high order with the respective series expansions of the exact functions $\overline{W}(\Lambda,y)$ for $\Lambda=(6^3)$ [to $O(y^{10})$] and for $\Lambda=(4\cdot 8^2)$ [to at least $O(y^{12})$], is not restricted to just these lattices. Indeed, we observe that for both of the lattices $(3\cdot 12^2)$ and $(4\cdot 6\cdot 12)$, the respective small-y series for the lower bound and the exact function coincide to at least to $O(y^{13})$ and $O(y^{11})$, respectively [41]. Thus, in general, this establishes that for a number of lattices our rigorous lower bounds actually serve as quite good approximations to the exact W functions, especially for large q.

VII. PLOTS OF $W_r(\Lambda,q)$ AND $\overline{W}(\Lambda,y)$

In Fig. 6 we plot $W_r(\Lambda,q)=q^{-1}W(\Lambda,q)$ for the eleven Archimedean lattices, for $y=1/(q-1)$ in the range $0\leqslant y\leqslant 0.30$, corresponding to q greater than about 4. We have evaluated these from our small-y series expansions of $\overline{W}(\Lambda,y)$ together with the definition (4.5). We find that $W_r(\Lambda,q)$, $W(\Lambda,q)$, and hence the ground-state entropy of the q-state Potts antiferromagnet $S_0(\Lambda,q)=k_B\ln W(\Lambda,q)$ are monotonically decreasing functions of the coordination number $\Delta(\Lambda)$ of the lattice Λ. This is a consequence of the fact that as one increases Δ, one increases the number of constraints restricting the coloring of each vertex of the lattice. Indeed, one can observe, especially for small y, that the eleven curves in Fig. 6 fall into four groups for the four values of $\Delta=3$, 4, 5, and 6. For further analytical purposes, we include also a plot of the reduced function $\overline{W}(\Lambda,y)$ in Fig. 7. Again, this is calculated from our small-y series. From our detailed comparison of lower bounds and small-y series for the homopolygonal lattices and the $(4\cdot 8^2)$ lattice

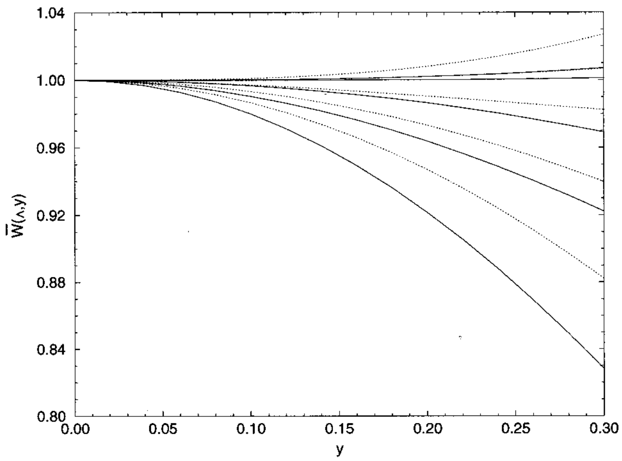

FIG. 7. Plots of $\overline{W}(\Lambda,y)$ as a function of $y=1/(q-1)$ for Archimedean lattices Λ. For visual clarity, the curves are shown alternately as solid (s) and dotted (d). The order of the curves, from bottom to top, is (3^6) (s), $(3^4\cdot 6)$ (d), $(3^3\cdot 4^2)$ (s), $(3\cdot 6\cdot 3\cdot 6)$ (d), $(3\cdot 12^2)$ (s), $(3\cdot 4\cdot 6\cdot 4)$ (d), (6^3) (s), $(4\cdot 8^2)$ and $(4\cdot 6\cdot 12)$ as almost coincident dotted and solid curves, and, finally, (4^4) (d). See the text for further details.

with Monte Carlo calculations, we expect that these curves are accurate over the range shown, i.e., $y=0$ to $y=0.3$. We have also checked this by evaluating the sizes of the highest calculated terms in our series.

We note the following theorem.

Theorem. If a lattice Λ' can be obtained from another Λ by connecting disjoint vertices of Λ with bonds, then $W(\Lambda',q)\leqslant W(\Lambda,q)$ (where $q\geqslant 0$ is an integer). For $q\leqslant \max\{q_c(\Lambda),q_c(\Lambda')\}$, this inequality applies to the W functions defined with the D_{nq} order of limits in Eq. (4.3), while for larger q, it applies to either of the definitions (4.3) and (4.2) since they are equivalent for this latter range of q.

Proof. Consider a finite, n-vertex lattice of type Λ, denoted Λ_n. We use the addition-contraction theorem from graph theory, the statement of which is the following. Let G be a graph and consider any two vertices v,v' on G that are not adjacent, i.e., not connected by a bond of G. Denote the graph with a bond connecting v and v' as $G_{v-b-v'}$ and the graph with these two vertices identified as $G_{v=v'}$. Then $P(G,q)=P(G_{v-b-v'},q)+P(G_{v=v'},q)$. Since $P(G_{v=v'},q)\geqslant 0$, it follows that $P(G_{v-b-v'},q)\leqslant P(G,q)$. Now take $\Lambda_n=G$ and add bonds as necessary to construct the lattice Λ'_n. Each time one adds a bond, one gets an inequality on the corresponding chromatic polynomials, thereby producing a sequence of such inequalities, expressing the fact that the chromatic polynomial for the original lattice is greater than or equal to that for the lattice with one bond added, which is greater than or equal to that for the lattice with two bonds added, etc. Together, these yield the inequality $P(\Lambda_n,q)\geqslant P(\Lambda'_n,q)$. Now let $n\to\infty$ to obtain $W(\Lambda,q)_{D_{nq}}\geqslant W(\Lambda',q)_{D_{nq}}$. For $q>\max\{q_c(\Lambda),q_c(\Lambda')\}$, both of these definitions are equivalent, so one can drop the subscripts D_{nq} and D_{qn}.

We give two examples of this theorem. (Subscripts indicating orders of limits in the definition of W are understood where necessary.) First, as recalled above, the square lattice can be obtained from the honeycomb lattice by such bond addition and consequently, $W((4^4),q)\leqslant W((6^3),q)$. Second, the triangular lattice can be obtained from the square lattice by bond addition, so $W((3^6),q)\leqslant W((4^4),q)$.

Concerning the plot of $\overline{W}(\Lambda,y)$, we observe one basic feature: As y increases from 0, i.e., q decreases from ∞, the initial behavior of $\overline{W}(\Lambda,y)$ can be understood as resulting from the leading term in the small-y expansion

$$\overline{W}(\Lambda,y)=1+(-1)^g\nu_g y^{g-1}+\cdots, \tag{7.1}$$

where g denotes the girth of Λ. That is, for even (odd) g, $\overline{W}(\Lambda,y)$ increases (decreases).

It is of interest to compare our results for the dependence of the $W(\Lambda,q)$ coloring function or, equivalently, the exponent of the ground-state entropy of the Potts antiferromagnet on the lattice coordination number Δ with the Δ dependence of other models that exhibit ground-state entropy. We first consider the (spin-1/2) Ising antiferromagnet (IAF) on the triangular and kagomé lattices. The exact solutions in these cases yield [5]

$$\begin{aligned} S_0(\mathrm{IAF},(3^6))/k_B &= \frac{1}{2}\int_0^{2\pi}\frac{d^2\theta}{(2\pi)^2}\ln(3+2P) \\ &= \frac{2}{\pi}\int_0^{\pi/3} d\omega \ln(2\cos\omega) \\ &\simeq 0.3231 \end{aligned} \tag{7.2}$$

for the triangular lattice, where

$$P=\cos(\theta_1)+\cos(\theta_2)+\cos(\theta_1+\theta_2), \tag{7.3}$$

and for the kagomé lattice [25]

$$S_0(\mathrm{IAF},(3\cdot 6\cdot 3\cdot 6))/k_B=\frac{1}{6}\int_0^{2\pi}\frac{d^2\theta}{(2\pi)^2}\ln(21-4P)\simeq 0.5018. \tag{7.4}$$

Thus, although the ground-state entropy is accompanied by frustration in these cases, in contrast to the q-state Potts antiferromagnet for the range $q\geqslant\chi(\Lambda)$ considered in the rest of this paper, it is again true that the ground-state entropy decreases as the coordination number Δ of the lattice increases. A similar dependence has been reported in the case of the quantum Heisenberg antiferromagnet; for the cases where this model involves frustration, recent studies indicate that it has a ground state with long-range order (albeit nonmaximal) on the triangular lattice, but with nonzero ground-state entropy and no long-range order in the case of the kagomé lattice [23].

We also make a comparison with the Δ dependence of generalized ice models. At normal pressures $p\sim 1$ atm, ice forms a wurzite crystal with fixed coordination number $\Delta=4$, so, of course, one cannot vary Δ in a realistic ice model. A very accurate estimate of the entropy of ice was obtained by Pauling [2]: $S_0(\mathrm{ice})_{P,molar}/R=\ln(3/2)=0.4055$, where, as above, $R=N_{Avog}k_B$, to be compared with the measured value of $S_0/R=0.41\pm 0.03$ [1]. Although one cannot vary Δ

for real ice itself at $p=1$ atm, one can consider an abstract statistical model constructed to have two-valued variables (say arrows) assigned to links subject to the constraint of local arrow conservation, inspired by the physical and chemical constraint of local electric neutrality in real ice. Clearly, such models can only be defined on a lattice with even coordination number Δ. One sees that this immediately constitutes a difference with spin models, which can be defined on lattices with even or odd Δ, as well as lattices such as the dual Archimedean lattices on which different vertices v_i have different degrees Δ_i. We recall that there is a straightforward generalization of the Pauling estimate for the exponential of the entropy of real ice to that for an abstractly defined ice-type model; this consists of the product 2^E describing the unconstrained number of positions of the hydrogen ions on the bonds [where $E=(\Delta/2)V$ and V denotes the number of vertices on the lattice], multiplied by a reduction factor, which is the fraction of the number of configurations for each vertex (oxygen location) that satisfy local electric neutrality. For each vertex this fraction is

$$\binom{\Delta}{\Delta/2} \Big/ 2^{\Delta},$$

so combining these two factors yields the generalized Pauling estimate for the exponent of the entropy, per site, for ice-type models (denoted by a subscript I),

$$W_I(\Lambda)_P = 2^{-\Delta/2}\binom{\Delta}{\Delta/2}. \tag{7.5}$$

This is a monotonically increasing function of (even) Δ. Since Eq. (7.5) is known to be a rigorous lower bound on $W_I(\Lambda)$ [42], it follows that $W_I(\Lambda)$ is also a monotonically increasing function of (even) Δ. This shows that different models that both exhibit nonzero ground state entropy, such as (i) the zero-temperature Potts antiferromagnets for $q \geqslant \chi(\Lambda)$ on various lattices Λ; the (frustrated) Ising antiferromagnet, and the (frustrated) quantum Heisenberg antiferromagnet on the triangular and kagomé lattices on the one hand and (ii) ice-type models, on the other hand, can have quite different dependences on lattice properties such as the coordination number Δ.

VIII. CHROMATIC ZEROS AND SUPPORT FOR A CONJECTURE FOR REGULAR LATTICES

We have calculated chromatic polynomials for finite sections of heteropolygonal Archimedean lattices and for several Laves lattices and in each case have calculated the zeros of these polynomials, i.e., the respective chromatic zeros for these lattices. We have also done this for the simple cubic lattice. Our main motivation for these calculations is to check whether the results are consistent with the conjecture that we made previously [20], namely, that a sufficient condition that $W_r(\{G\},q)$ be analytic at $1/q=0$, [i.e., that the region boundary $\mathcal{B}$ separating different regions where $W(\{G\},q)$ is analytic does not have any components that extend to complex infinity in the q plane] is that $\{G\}$ is a regular lattice. (This is not a necessary condition; as our exact results in Ref. [17] showed, there are many families of

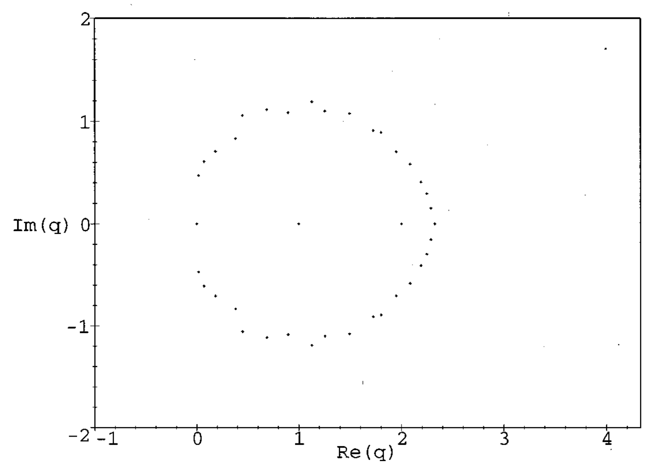

FIG. 8. Chromatic zeros for a section of the $(3\cdot 12^2)$ lattice, with $n=48$ vertices.

graphs that are not regular lattices but do have compact region boundaries $\mathcal{B}$.) In Refs. [17,20] we compared the chromatic zeros for various families of graphs with exact results on the $n\to\infty$ limits of these graphs and the corresponding $W(\{G\},q)$ functions, where $\{G\}$ denotes the $n\to\infty$ limit of n-vertex graphs of type G. As we discussed, as $n\to\infty$, the chromatic zeros (aside from a well-understood discrete subset including zeros at $q=0,1$ and, for graphs containing at least one triangle, also $q=2$) merge to form boundary curves $\mathcal{B}$ that separate regions of the complex q plane in which $W(\{G\},q)$ takes on different analytic forms. For finite graphs, these chromatic zeros lie near, or for some families of graphs [17] exactly on, the asymptotic boundary curves $\mathcal{B}$. However, for cases where $\mathcal{B}$ does have components extending to complex infinity in the q plane, we found that the chromatic zeros calculated on finite lattices deviate strongly from the parts of $\mathcal{B}$ that extend to infinity (see also [43]). In particular, as one increases the lattice size, one finds that the (complex-conjugate) complex chromatic zeros farthest from the real axis in the q plane move farther away from this axis. This then serves as a means by which one can infer, from calculations of chromatic zeros on finite lattices, whether the corresponding region boundaries $\mathcal{B}$ have components that extend to complex infinity in cases where one does not have exact solutions for $W(\{G\},q)$ in $n\to\infty$ limit available. As we have discussed before [17,20], exact results for the triangular lattice and chromatic zeros calculated on finite square and honeycomb lattices [14] yield boundary curves $\mathcal{B}$ that satisfy our conjecture. Summarizing our results for various Archimedean and dual Archimedean lattices, and for the simple cubic lattice, we find in all cases that the chromatic zeros are consistent with our conjecture in Ref. [20]. We show two typical examples in Figs. 8 and 9. In both cases, we use free boundary conditions and choose sections of the lattice that have comparable lengths in the x and y directions.

From our earlier comparisons of chromatic zeros for various families of graphs with the exact region boundaries $\mathcal{B}$ calculated in the limit of infinitely many vertices [17,20], we know that it is possible to make some reliable inferences about these boundaries from the positions of the chromatic zeros for finite lattices. Indeed, a subset of these chromatic zeros merges to form the boundaries $\mathcal{B}$ in this limit. (There

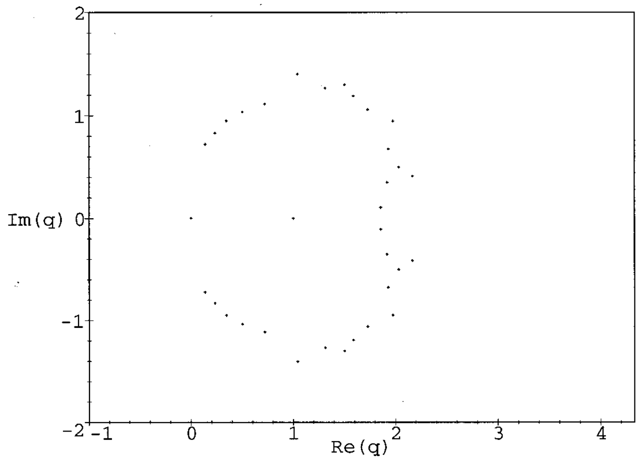

FIG. 9. Chromatic zeros for a section of the $(4\cdot 8^2)$ lattice, with $n=36$ vertices.

are also discrete isolated chromatic zeros such as those at $q=0,1$ and, if Λ contains triangles, also at $q=2$.) Our calculations of chromatic zeros for Archimedean lattices and their duals in two dimensions and for the simple cubic lattice are consistent with the inference that in the thermodynamic limit, (i) the respective boundaries separate the complex q plane into at least two regions, one of which (denoted R_1 in Refs. [17,20]) includes the positive real q axis extending to $q=\infty$ and the circle at complex infinity, i.e., the image under inversion of the origin in the $1/q$ plane and (ii) the outermost component of the boundary $\mathcal{B}$ intersects the real q axis on the left at $q=0$ (for all Λ) and on the right at the point that we have denoted $q_c(\Lambda)$. Further studies on larger lattices will help to elucidate the detailed shapes of the boundaries $\mathcal{B}$ for various lattices. For example, using sufficiently large lattices together with comparisons of chromatic zeros for different lattices sizes to measure finite-size shifts of these zeros, one can carry out an extrapolation to the thermodynamic limit to determine the value of $q_c(\Lambda)$ with reasonable accuracy. Work on this is in progress.

IX. CONCLUSION

The subject of nonzero ground-state entropy is a fundamental one in statistical mechanics. In this paper we have proved a general rigorous lower bound for $W(\Lambda,q)$, the exponent of the ground-state entropy of the q-state Potts antiferromagnet on an arbitrary Archimedean lattice. The function $W(\Lambda,q)$ is also of considerable interest in mathematics, in particular, the coloring of (finite) graphs and their infinite-n limits. From calculations of large-q series expansions for the exact $\overline{W}(\Lambda,y)$ functions and comparison with our lower bounds on the various Archimedean lattices Λ, we have shown that the lower bounds are actually very good approximations to the exact functions for large q. We have also calculated lower bounds and series for the duals of Archimedean lattices. Finally, from calculations of chromatic zeros on a number of lattices, we have obtained further evidence for the conjecture that a sufficient condition for $q^{-1}W(\Lambda,q)$ to be analytic at $1/q=0$ is that Λ is a regular lattice.

ACKNOWLEDGMENT

This research was supported in part by NSF Grant No. PHY-93-09888.

[1] W. F. Giauque and J. W. Stout, J. Am. Chem. Soc. **58**, 1144 (1936).
[2] L. Pauling, *The Nature of the Chemical Bond* (Cornell University Press, Ithaca, 1960), p. 466.
[3] N. G. Parsonage and L. A. K. Staveley, *Disorder in Crystals* (Oxford University Press, New York, 1978).
[4] P. W. Atkins, *Physical Chemistry* (Freeman, San Francisco, 1994), p. 710.
[5] G. H. Wannier, Phys. Rev. **79**, 357 (1950).
[6] K. Kano and S. Naya, Prog. Theor. Phys. **10**, 158 (1953).
[7] R. B. Potts, Proc. Camb. Philos. Soc. **48**, 106 (1952).
[8] C. M. Fortuin and P. W. Kasteleyn, Physica **57**, 536 (1972).
[9] F. Harary, *Graph Theory* (Addison-Wesley, Reading, MA, 1969).
[10] N. L. Biggs, *Algebraic Graph Theory*, 2nd ed. (Cambridge University Press, Cambridge, 1993).
[11] W. T. Tutte, *Graph Theory*, Vol. 21 of *Encyclopedia of Mathematics and its Applications*, edited by G. C. Rota (Addison-Wesley, New York, 1984).
[12] R. C. Read and W. T. Tutte, in *Chromatic Polynomials*, edited by L. W. Beineke and R. J. Wilson, Selected Topics in Graph Theory, 3 (Academic, New York, 1988).
[13] E. H. Lieb, Phys. Rev. **162**, 162 (1967).
[14] R. J. Baxter, J. Phys. A **20**, 5241 (1987).
[15] F. Y. Wu, Rev. Mod. Phys. **54**, 235 (1982); R. J. Baxter, J. Math. Phys. (N.Y.) **11**, 784 (1970).
[16] R. Shrock and S.-H. Tsai, J. Phys. A **30**, 495 (1997).
[17] R. Shrock and S.-H. Tsai, Phys. Rev. E **55**, 5165 (1997); **55**, 5184 (1997).
[18] R. Shrock and S.-H. Tsai, Phys. Rev. E **55**, 6791 (1997).
[19] R. Shrock and S.-H. Tsai, Phys. Rev. E **56**, 2733 (1997).
[20] R. Shrock and S.-H. Tsai, Phys. Rev. E **56**, 3935 (1997).
[21] A. P. Ramirez, G. P. Espinosa, and A. S. Cooper, Phys. Rev. Lett. **64**, 2070 (1990); C. Broholm , G. Aeppli, G. P. Espinosa, and A. S. Cooper, *ibid.* **65**, 3173 (1990).
[22] A. S. Wills, A. Harrison, S. A. M. Mentink, T. E. Mason, and Z. Tun, cond-mat/9607106.
[23] C. Zeng and V. Elser, Phys. Rev. B **42**, 8436 (1990); R. R. P. Singh and D. Huse, Phys. Rev. Lett. **68**, 1766 (1992); N. Elstner, R. R. P. Singh, and A. P. Young, *ibid* **71**, 1629 (1993; N. Elstner and A. P. Young, Phys. Rev. B **50**, 6871 (1994).
[24] J. Stephenson, J. Math. Phys. (N.Y.) **50**, 1009 (1964); **11**, 420 (1970).
[25] A. Süto, Z. Phys. B **44**, 121 (1981); Helv. Phys. Acta **54**, 191 (1981); **54**, 201 (1981).
[26] G. D. Birkhoff, Ann. Math. **14**, 42 (1912).
[27] H. Whitney, Ann. Math. **33**, 688 (1932); Bull. Am. Math. Soc. **38**, 572 (1932).

[28] G. D. Birkhoff and D. C. Lewis, Trans. Am. Math. Soc. **60**, 355 (1946).

[29] B. Grünbaum and G. Shephard, *Tilings and Patterns* (Freeman, New York, 1987).

[30] V. Matveev and R. Shrock, J. Phys. A **28**, 5235 (1995).

[31] F. Laves, Z. Kristallogr. **73**, 202 (1930); **78**, 208 (1931).

[32] K. I. Appel, W. Haken, and J. Koch, Illinois J. Math. **21**, 429 (1977); K. I. Appel and W. Haken, *ibid.*, **21**, 491 (1977).

[33] Our results for $\chi(\Lambda)$ are not difficult to obtain, although we have not been able to find them in the mathematical literature on graph theory, which deals mostly with proper (finite) graphs.

[34] N. L. Biggs, Bull. London Math. Soc. **9**, 54 (1977).

[35] See, e.g., P. Lancaster and M. Tismenetsky, *The Theory of Matrices, with Applications* (Academic, New York, 1985); H. Minc, *Nonnegative Matrices* (Wiley, New York, 1988).

[36] D. London,Duke Math. J. **33**, 511 (1966).

[37] The complete graph K_r is defined as the graph consisting of r vertices each of which is connected to all of the others with bonds.

[38] The lower bound $W_r(\Lambda,q)_{\ell} \equiv q^{-1}W(\Lambda,q)_{\ell}$ for the reduced function $W_r(\Lambda,q)$ of Eq. (4.4) is not, in general, monotonically increasing over this range $q \geqslant \chi(\Lambda)$, although $\lim_{q\to\infty} W_r(\Lambda,q)_{\ell} = \lim_{q\to\infty} W_r(\Lambda,q) = 1$.

[39] In passing, we note also that from $P(C_{2k+1},q=2) = 0$ and Eq. (4.12), it follows that $D_{2k+1}(q=2)=0$ for $k=1,2,\ldots$.

[40] J. F. Nagle, J. Combin. Theory **10**, 42 (1971); see also G. A. Baker, Jr., *ibid.* **10**, 217 (1971).

[41] Although we have only listed our small-y series for $\overline{W}((3\cdot 12^2),y)$ to $O(y^{13})$ and this coincides with all terms of the corresponding expansion of our lower bound $W((3\cdot 12^2),y)_{\ell}$, a preliminary calculation (unpublished) of higher orders of the series for $\overline{W}((3\cdot 12^2),y)$ indicates that this agreement continues for several more orders.

[42] L. Onsager and M. Dupuis, in *Rendiconti, Proceedings of the International School of Physics* ''Enrico Fermi,'' Course 10, *Bologna, 1960*, edited by N. Zanichelli (Italian Physical Society, Bologna, 1960). E. H. Lieb and F. Y. Wu in *Phase Transitions and Critical Phenomena*, edited by C. Domb and M. S. Green (Academic, New York, 1972), Vol. 1, p. 331.

[43] R. C. Read and G. F. Royle, *Graph Theory, Combinatorics, and Applications* (Wiley, New York, 1991), Vol. 2, p. 1009.